

Synthesis, Biological Activity, Molecular Docking Studies of a Novel Series of 3-Aryl-7*H*-thiazolo[3,2-*b*]-1,2,4-triazin-7-one Derivatives as the Acetylcholinesterase Inhibitors

Zhe Jin, Chao Zhang, Miao Liu, Simeng Jiao, Jing Zhao, Xiaoping Liu, Huangquan Lin, David Chi-cheong Wan & Chun Hu

To cite this article: Zhe Jin, Chao Zhang, Miao Liu, Simeng Jiao, Jing Zhao, Xiaoping Liu, Huangquan Lin, David Chi-cheong Wan & Chun Hu (2020): Synthesis, Biological Activity, Molecular Docking Studies of a Novel Series of 3-Aryl-7*H*-thiazolo[3,2-*b*]-1,2,4-triazin-7-one Derivatives as the Acetylcholinesterase Inhibitors, Journal of Biomolecular Structure and Dynamics, DOI: [10.1080/07391102.2020.1753576](https://doi.org/10.1080/07391102.2020.1753576)

To link to this article: <https://doi.org/10.1080/07391102.2020.1753576>

 View supplementary material 

 Accepted author version posted online: 08 Apr 2020.

 Submit your article to this journal 

 View related articles 

 View Crossmark data 

Synthesis, Biological Activity, Molecular Docking Studies of a Novel Series of 3-Aryl-7*H*-thiazolo[3,2-*b*]-1,2,4-triazin-7-one Derivatives as the Acetylcholinesterase Inhibitors

Zhe Jin¹, Chao Zhang¹, Miao Liu¹, Simeng Jiao¹, Jing Zhao¹, Xiaoping Liu^{1,*}, Huangquan Lin²,
David Chi-cheong Wan², Chun Hu^{1,*}

¹Key Laboratory of Structure-based Drug Design & Discovery, Ministry of Education; Shenyang Pharmaceutical University, Shenyang 110016, China

²School of Biomedical Sciences, Faculty of Medicine, The Chinese University of Hong Kong, Hong Kong SAR, China

*Correspondences: Xiaoping Liu & Chun Hu, Key Laboratory of Structure-based Drug Design & Discovery, Ministry of Education; Shenyang Pharmaceutical University, Shenyang 110016, China.

Emails: lxp19730107@163.com (X. Liu) & chunhu@syphu.edu.cn (C. Hu).

ABSTRACT

The acetylcholinesterase inhibitors play a critical role in the drug therapy for Alzheimer's disease. In this study, twenty-nine novel 3-aryl-7*H*-thiazolo[3,2-*b*]-1,2,4-triazin-7-one derivatives were synthesized and assayed for their human acetylcholinesterase (*hAChE*) inhibitory activities. Inhibitory ratio values of seventeen compounds were above 55 % with **4c** having the highest value as 77.19 %. The compounds with the halogen atoms in the aromatic ring, and *N,N*-diethylamino or *N,N*-dimethylamino groups in the side chains at C-3 positions exhibited good inhibitory activity. SAR study was carried out by means of molecular docking technique. According to molecular docking results, the common interacting site for all compounds were found to be peripheral anionic site whereas highly active compounds were interacting with the catalytic active site too.

KEYWORDS: Heterocycle; Thiazolo[3,2-*b*]-1,2,4-triazine; Synthesis; Acetylcholinesterase Inhibitor; SAR; Docking

HIGHLIGHTS:

1. A novel series of 3-aryl-7*H*-thiazolo[3,2-*b*]-1,2,4-triazin-7-one derivatives were synthesized and assayed for their human acetylcholinesterase (*hAChE*) inhibitory activities.
2. The SAR study of the target 3-aryl-7*H*-thiazolo[3,2-*b*]-1,2,4-triazin-7-one derivatives was summarized.
3. The active sites in the acetylcholinesterase were analyzed by molecular docking technique.

1. INTRODUCTION

As Alzheimer's disease (AD) was first reported in 1907, the number of people with AD has increased rapidly with the life span of human beings increasing. The pathogenesis of Alzheimer's disease (AD) is very complicated, it is generally believed that AD ascribed to multiple factors, including age, environment and heredity (Eckert et al., 2003; Pascoini, 2019; Rego & Oliveira, 2003). The acetylcholinesterase (AChE) inhibitors play an important role in drug therapy for AD. So far, there are only five drugs for AD treatment approved by the FDA (U.S. Food and Drug Administration) - four are AChE inhibitors, including tacrine, donepezil, rivastigmine, galantamine, and one *N*-methyl-D-aspartic acid (NMDA) receptor antagonist memantine (Eslami, Nezafat, Negahdaripour, & Ghasemi, 2019; Shamsi, et al., 2020; Zheng, Fridkin, & Youdim, 2010). Among them, tacrine has been discontinued in the US in 2013, due to hepatotoxicity (Atienzar, et al., 2016). In addition, huperzine A has been approved by China National Medical Products Administration (CNMPA). On November 2, 2019, CNMPA approved carbohydrate based drug GV-971 for treating AD. The drug can restore the balance of intestinal flora, reduce the accumulation of peripheral related metabolites phenylalanine/isoleucine, and improve the cognitive impairment (NMPA, 2019).

Even though AChE inhibitors play an important role in drug therapy for AD, the drugs can only reduce symptoms and, to some extent, improve quality of life. There are still no effective drugs to prevent, improve or reverse the occurrence of AD. The development of drug is a time-consuming, expensive, and interdisciplinary process, which involves medicinal chemistry, pharmacology, pharmacokinetics and clinical trials (de Almeida, et al., 2019; Taft, V. da Silva, & C. da Silva, 2008). The average cost of a newly marketed drug in the USA is \$500 million to \$800 million, and it takes 11 to 15 years. Several different computer-aided drug design (CADD) techniques have been used to

speed up the drug development process (Ece, & Sevin, 2010; Ece, 2020; Śledź, & Caflisch, 2018; Neto, 2017; Taft, et al., 2008; Tahtaci, Karacık, Ece, Er, & Şeker, 2017). These included molecular docking, pharmacophore model building, physicochemical and ADME properties calculation, drug target identification, structure-activity relationships (SAR) explanation. In this study, the structure of AChE, AChE-ligand interactions and related active sites are analyzed by using CADD technology to develop new and effective AD lead compounds.

By the end of September 2019, there are 206 AChE crystal structures in Research Collaboratory for Structural Bioinformatics Protein Data Bank (RCSB PDB). Among them, 87 came from *Torpedo californica* (*Torpedo californica* AChE, *TcAChE*), 72 came from *Mus musculus* (mouse AChE, *mAChE*), and 39 came from *Homo sapiens* (human AChE, *hAChE*). The *hAChE*-donepezil complex (PDB code 4EY7, solved at 2.3509 Å) (Cheung, et al., 2012) and the *TcAChE*-donepezil complex (PDB code 1EVE, solved at 2.5 Å) (Kryger, Silman, & Sussman, 1999) have been superimposed to observe the differences, especially the residues of the region near the active site of AChE. There are significant differences between the binding sites of *hAChE* and *TcAChE*, which lead to the binding of donepezil in different conformations. In this study, the *hAChE*-ligand complex was selected for docking (Cheung, et al., 2012).

The most remarkable feature of the structure of AChE is a deep and narrow gorge, about 20 Å long, the cavity is called 'active-site gorge'. The catalysis active site (CAS), first discovered, is the most important site for activity. It is located at the bottom of the active-site gorge and consists of Ser200, Glu327, and His440 in *TcAChE* (Dvir, Silman, Harel, Rosenberry, & Sussman, 2010; Sussman, et al., 1991). The peripheral anionic site (PAS) is located near the entrance of the gorge and consists of Tyr70, Asp72, Tyr121, Glu278, Trp279 and Tyr334, and some small molecule inhibitors block the entrance of the active-site gorge to exert the inhibitory effects (Khalid, et al., 2010; Shiri, Pirhadi, & Ghasemi, 2019; Wan, et al., 2020). In 2005, a series of tacrine-indole heterodimers were found to display excellent AChE inhibition, with IC₅₀ value of 20 pM on AChE (Muñoz-Ruiz, et al., 2005). Molecular docking results showed other sites participated in the interactions. The quaternary ammonium binding site (QABS) consists of Trp84, Tyr130, Glu199, and Phe330, and is located between CAS and PAS (Harel, Quinn, Nair, Silman, & Sussman, 1996; Khalid, et al., 2010; Kryger, et al., 1999; Wan, et al., 2020). The amino acid residues of *TcAChE*

active sites (PDB ID: 1FSS) (Harel, Kleywegt, Ravelli, Silman, & Sussman, 1995), including CAS, PAS and QABS; and the residues of *hAChE* active sites (PDB ID: 2X8B) (Carletti, et al., 2010) are shown in Figure 1. Each color in the Figures was represented one active site: CAS for green, PAS for blue violet, and QABS for deep pink.

AChE inhibitors, on the market interact with different active sides of the AChE. They are listed in Table 1.

Table 1 shows that AChE inhibitors interact with CAS, PAS and QABS, and each of them except rivastigmine, interacts with at least two kinds of active sites. Based on these, twenty-nine 3-aryl-7*H*-thiazolo[3,2-*b*]-1,2,4-triazin-7-one derivatives were designed and synthesized, their AChE inhibitory activities were evaluated, and the active sites of the target compounds were calculated by molecular modeling.

2. MATERIALS AND METHODS

2.1. Chemistry

The synthetic strategy to prepare the target compounds is illustrated in Schemes 1-2.

All reagents and solvents were purchased from common commercial suppliers and were used without further purification unless otherwise indicated. Melting points were taken on a Koffler hot-plate apparatus and were uncorrected. Mass spectra (MS) were obtained using an electronic impact (EI) ion source at 70 eV in an Agilent spectrometer (with direct insertion probe) or with an electrospray (ESI) ion source in a Waters spectrometer at 3.5 kV spray voltage, acetonitrile was used as the solvent. ¹H NMR spectra were determined on a Bruker spectrometer operating at 300 MHz or 400 MHz or 600 MHz with TMS as the internal standard, and DMSO-*d*₆ or CDCl₃ was used as solvent. The IR spectra were recorded on a Bruker AFS55 spectrometer.

The styrene derivatives were synthesized according to the previous publications (Marvel, & Schertz, 1943). The styrene derivatives reacted with KMnO₄ alkaline aqueous solution, and hydrochloric acid was added to acidify the reaction solution to produce keto acids **1**. Compounds **2** were prepared by using compound **1** reacted with thiosemicarbazide in sodium hydroxide aqueous solution. The target compounds **3a-3h** were obtained by a condensation reaction of compounds **2** with substituted phenacyl chlorides in acetic acid. The target compounds **4a-4e** were prepared by **3f-3h** with substituted alkyl chloride by Williamson reaction shown in Scheme 1 (Jin, et al., 2010a;

Jin, et al., 2010b).

The 4-arylmethylideneoxazol-5(4*H*)-ones **5** were easily converted from the aromatic aldehydes by cyclization. Then, the hydrolysis of **5** in the acetone aqueous solution resulted in α -(acetylamino)cinnamic acids **6**, subsequently, **6** were converted to aryl pyruvic acids **7** by treatment with diluted hydrochloric acid. Compounds **7** reacted with thiosemicarbazide to give the cyclized products 3-thioxo-1,2,4-triazin-5(2*H*)-ones **8**. The target compounds **9a-9d** were prepared by a condensation reaction of compounds **8** with substituted phenacyl chlorides in acetic acid. The target compounds **10a-10l** could be obtained with Williamson reaction shown in Scheme 2 (Liu, et al., 2009; Liu, Shang, Shi, Wan, & Lin, 2014).

2.2. *hAChE* activity assay

The *hAChE* inhibitory activity values of the tested target compounds were evaluated by means of Ellman's test method (Ellman, Courtney, Andres, & Featherstone, 1961; Liu, et al., 2009; Liu, et al., 2010; Liu, et al., 2013; Liu, et al., 2014; Malinak, et al., 2020; Mosmann, 1983; Xu, et al., 2012). The *hAChE* stock solution was prepared by dissolving *hAChE* 0.5 unit in 100 mM phosphate buffered saline (PBS) buffer (pH 7.4). The tested target compounds (10 mM) were dissolved in DMSO. The assay solution consisted of 100 mM PBS buffer (pH 7.4), 10 mM 5,5'-dithiobis-(2-nitrobenzoic acid) (DTNB, Ellman's reagent), 5 mL *hAChE*, 10 mL drug (the tested target compounds or positive control huperzine-A), and 12.5 mM acetylthiocholine iodide (ATCh) water solution. The final assay volume was 900 μ L. The tested target compounds were incubated the reaction at 37 °C for 15 min with continuous gentle shake, added 50 μ L ATCh and 50 μ L DTNB, incubated at 37 °C for about 20 min with continuous gentle shake, waited until the yellow color developed. The absorbance values were measured at 412 nm, and the inhibition values were calculated.

2.3. Computational Methods

The protein structure was obtained from the crystallographic complex of human AChE in complex with fasciculin-II (RCSB PDB ID: 2X8B), the resolution value of the complex crystal was 2.95 Å (Carletti, et al., 2010); and the complex of human AChE in complex with donepezil (RCSB PDB ID: 4EY7), the resolution value of the complex crystal was 2.3509 Å (Cheung, et al., 2012).

The complexes were prepared by Schrödinger's protein preparation wizard, which removed the hetero atoms and water molecules from the protein, built the missing side chain atoms, corrected the structure of the protein and added hydrogen atoms before docking (Shivakumar, et al., 2010). Afterwards, the OPLS_2005 force field was used to optimize protein energy and eliminate steric hindrance (Itteboina, Ballu, Sivan, & Manga, 2017). The positions of the native ligand was defined to generate grid for subsequent molecular docking work (Wang, et al., 2018).

The Molegro Virtual Docker (MVD) software version 4.1.0 was used for the molecular docking process (Han, Lai, & Du, 2014; Khan, Fuskevåg, & Sylte, 2009; Vaqué, et al., 2008), the interactions between *hAChE* and the ligands were calculated by using Lamarckian Genetic Algorithm, the grid resolution was 0.3 Å, the binding site radius was 15 Å, and other parameters were all default values. All the compounds were docked into the active sites of *hAChE* (PDB code 2X8B and 4EY7). The complexes of ligand-receptor were viewed by Discovery Studio ViewerPro ViewerLite50 program (Kangueane, & Nilofer, 2018; Yang, 2010; Zhu, Wang, Li, Han, & Zhao, 2017).

3. RESULTS AND DISCUSSION

3.1 Chemistry

The structures of all the target compounds are listed in Table 2. The structures of all the newly synthesized compounds were characterized by ¹H-NMR, MS, and IR. The synthetic procedures, experimental details and spectra data for the target compounds are available as the supplementary material.

2.2. Biological evaluation

Table 3 lists the *hAChE* inhibitory activity values of the target compounds, and the positive control drug was huperzine A (from synthetic, ≥98% (TLC), Sigma), 0.5 unit *hAChE* (Sigma C-1682) was used. Each was performed in thrice. The incubation time was 20 min. The assay procedures for the target compounds are available as the supplementary material.

Some of the target compounds exhibited good *hAChE* inhibitory activity, the inhibitory activity values of seventeen compounds were above 55 %, and the highest value of **4c** was 77.19 %.

All the target compounds were substituted in the aromatic rings and the side chains at C-3 and C-6 positions. On the whole, different substituted groups and side chains had great influences on AChE inhibitory activity. The target compounds of which the halogen atoms in the aromatic rings, and *N,N*-diethylamino groups, *N,N*-dimethylamino groups in the side chains at C-3 positions (compounds **3b**, **3c**, **3d**, **10e**, **10f**, **10h**, **10i**, **10k**), exhibited good inhibitory activity. The existence of morpholine rings at C-3 positions decreased the inhibitory activity (compounds **4b**, **4d**, **10e**, **10a**, **10g**).

2.3. Molecular docking

The model was obtained by docking ligand (the target compounds) to the *hAChE* (from RCSB PDB ID: 2X8B) using the methods we have described in section 2.4. Each of the target compounds was docked to simulate the hydrogen bonds interaction sites of the minimum energy conformation of the compounds. The detailed interactions for the target compounds are available as the supplementary material.

The internal validation of molecular docking was carried out. PDB ID of 4EY7 was selected to check the RMSD value. In the co-crystal complex structure of 4EY7, the ligand was donepezil. The native ligand in the complex and the docking ligand were overlapped for comparison (Figure 2). The RMSD value was 0.575 Å, which showed the molecular docking method was reliable.

The target compounds were classified into three groups in accordance to the *hAChE* inhibitory activity values of the compounds, highly active compounds (activity values > 55 %), moderately active compounds (activity values 55 % - 40 %) and inactive compounds (activity values < 40 %). The hydrogen bond interaction sites of the minimum energy conformation of the compounds are listed in Tables 4-6.

Table 4-6 show the interaction site in *hAChE* and the target compounds. For the seventeen group I compounds, the hydrogen bond interaction sites of the highly active compounds included at least two active sites: ten interacted with CAS and PAS; five interacted with CAS and QABS; two interacted with CAS, QABS and PAS. All included CAS active site. In group II, for the six moderately active compounds. Three compounds interacted with QABS and PAS. Another three only with PAS. In group III, for the six inactive compounds. Five compounds interacted with PAS, and one with QABS and PAS.

The active sites of *hAChE* and compounds **4a**, **4d** and **10g** are drawn in Figure 3.

In Figure 3, the three target compounds **4a**, **10g**, **4d** were embedded in the gorge no matter how different conformations of the compounds. The *hAChE* inhibitory activity value of **4a** was 58.12 %, because the compound was at the bottom of the gorge, and there was a hydrogen bond between Ser203 of CAS and **4a**. The inhibitory activity value of **10g** was 43.20 %. The compound was at the middle part of the gorge, and the hydrogen bonds were observed between QABS, PAS and **10g**. The inhibitory activity value of **4d** was only 10.65 %, because the compound was located at the upper part of the gorge, and the hydrogen bonds were available between PAS and **4d**.

All the minimum energy conformations of the target compounds are depicted in Figure 4 and Figure 5. The classified methods of the target compounds were in accordance to Table 2. The target compounds were divided into 3 groups in accordance with the *hAChE* inhibitory activity values of the compounds; above 55 %, below 40 %, and others.

Figure 4 shows that, most of the seventeen target compounds were embedded in the gorge no matter how different the conformations of the compounds were. All the compounds were at the bottom of the gorge, and there were hydrogen bonds between the target compounds and Ser203 of CAS.

Figure 5 shows that, most of the six target compounds were inserted into the middle deep of the gorge at similar conformations. Hydrogen bonds are observed between QABS, PAS and the target compounds.

Figure 6 shows all the six compounds scattered at the upper part of the gorge, and the hydrogen bonds interaction are available between PAS and the target compounds.

The hydrogen bond interaction sites of the twenty-nine target compounds are the same as compounds **4a**, **10g**, **4d**.

2.4 Verification for molecular docking

The molecular docking of the synthesized compounds was also carried out using X-ray crystal structure of *hAChE* in complexed with pharmacologically important ligand, Donepezil (PDB ID: 4EY7, 2.35 Å resolution). The docking results used 4EY7 are listed in Tables 7-9. The hydrogen bonds interaction sites, hydrogen bonds active sites, and other interactions sites are summarized. The same hydrogen bonds interaction sites and active sites as 2X8B were bold. The details are described as the supplementary material.

The verification results of *hAChE* (4EY7) showed that in group I, seventeen highly active compounds, the hydrogen bond interaction sites of seven compounds were at the catalytic active site (CAS), one was at CAS and the peripheral anionic site (PAS), three were at CAS and the quaternary ammonium binding sites (QABS); two were at CAS, QABS, PAS, and the thirteen out of seventeen included CAS active site.

In comparison, the results of *hAChE* (2X8B) showed that in group I, the hydrogen bond interaction sites included at least two active sites: ten with CAS and PAS; five with CAS and QABS; the other two with CAS, QABS and PAS, and all included CAS active site.

The verification results with *hAChE* (4EY7) showed that in group II, six moderately active compounds, the hydrogen bond interaction sites of four compounds were with QABS and PAS, and another two were with PAS only.

In comparison, the results with *hAChE* (2X8B) showed that in group II, the hydrogen bond interaction sites of three compounds were with QABS and PAS, and another three were with PAS only.

The verification results with *hAChE* (4EY7) showed that in group III, the six inactive compounds, the hydrogen bond interaction sites of four compounds were with PAS, and another two were with QABS and PAS.

In comparison, the results with *hAChE* (2X8B) showed that in group III, the hydrogen bonds interaction sites of five compounds were with PAS only, and another one was with QABS and PAS.

Based on above analysis in Tables 4-9, the crucial amino acid residues were identified as Ser203 in CAS, Trp86 and Tyr133 in QABS, Tyr72, Asp74, Tyr124, Glu202, Tyr337, Tyr341 in PAS.

Interaction of compounds with *hAChE* were analyzed to verify the involvement of the crucial amino acids found from molecular docking, the *hAChE*-ligand contact atlas (<https://www.mrc-lmb.cam.ac.uk/rajini/index.html>) and the binding interaction of ligands (analyzed by using Discovery Studio Visualizer v16.1.0.15350) of the three PDB (code 4EY5, ligand is (-)-huperzine A; code 4EY6, ligand is (-)-galantamine; code 4EY7, ligand is donepezil) were analyzed. The AChE-ligand contacts are represented by asteroid plot and 3-D binding interaction plot as shown in Figure 7 to Figure 9.

The asteroid plots of *hAChE* co-crystal structure and the binding interactions showed the following amino acid residues in *hAChE* are important for the interaction with compounds: Tyr72, Asp74,

Trp86, Gly120, Gly121, Gly122, Tyr124, Gly126, Tyr133, Glu202, Ser203, Trp286, Ser293, Phe295, Tyr337, Phe338, Tyr341, His447. Tyr72, Asp74, Trp86, Tyr124, Gly126, Ser203, Ser293, Phe295, Tyr337, His447 are especially crucial because there were hydrogen bonds between the compounds and AChE, Trp86, Gly121, Tyr124, Ser203, Tyr337, Phe338, Tyr341, His447 are made weak interactions with the compounds. The results are basically consistent with molecular docking.

3. CONCLUSION

The goal of this study was to synthesize a series of 3-aryl-7*H*-thiazolo[3,2-*b*]-1,2,4-triazin-7-one derivatives, to evaluate their *h*AChE inhibitory activities, and to study the structure-activity relationship by using molecular docking method.

Twenty-nine target compounds were synthesized, the structures of all the novel synthesized compounds were characterized by ¹H NMR, MS, and IR. All the target compounds exhibited *h*AChE inhibitory activity, the values of seventeen compounds were above 55 %, and the highest value of **4c** was 77.19 %.

The target compounds of which the halogen atoms in the aromatic rings, and *N,N*-diethylamino groups, *N,N*-dimethylamino groups in the side chains at C-3 positions exhibited good inhibitory activity. The existence of morpholine rings at C-3 positions decreased the inhibitory activity.

Most of the seventeen target compounds of which the *h*AChE inhibitory activity values were above 55 % were embedded in the active site gorge disregard the conformations of the compounds, these conformations were high incidence. Most of the compounds were docked into the bottom of the gorge, and there were hydrogen bonds between the compounds and Ser203 of CAS. Most of the six target compounds of which the *h*AChE inhibitory activity values were between 40 % and 55 % were inserted into the middle part of the gorge, and hydrogen bond interaction existed between QABS, PAS and the compounds. All the six compounds with *h*AChE inhibitory activity values below 40 % were only inserted into the upper part of the gorge, and hydrogen bond interaction existed between PAS and the compounds. Ser203 in CAS, Trp86 and Tyr133 in QABS, Tyr72, Asp74, Tyr124, Glu202, Tyr337, Tyr341 in PAS were crucial amino acid residues. The molecular docking results and confirmation of crucial amino acid residues have been verified by two *h*AChE-ligand co-crystal complexes.

ACKNOWLEDGMENT

This work was supported by the National Science Foundation of China (NSFC) for the grant No. 21072130 & 21342006; the Program for Innovative Research Team of the Ministry of Education of China (Grant No. IRT_14R36), the Natural Science Foundation of Liaoning Province, China for the grant No. 201602695 and 2019-ZD-0458; and the Scientific Research Foundation of Department of Education of Liaoning Province, China for the grant No. L2015517. The authors would like to thank Molegro ApS for kindly providing a free evaluation copy of their software package, Dassault Systèmes Biovia Co. for providing Discovery Studio Visualizer v16.1.0.15350, and Accelrys Co. for allowing the use of ViewerLite 5.0 software.

CONFLICT OF INTEREST

The authors declare that they have no competing interests.

FUNDING

National Science Foundation of China (NSFC) with grant No. 21072130 & 21342006.

REFERENCES

- Atienzar, F. A., Blomme, E. A., Chen, M., Hewitt, P., Kenna, J. G., Labbe, G., Moulin, F., Pognan, F., Roth, A. B., Suter-Dick, L., Ukairo, O., Weaver, R. J., Will, Y., & Dambach, D. M. (2016). Key challenges and opportunities associated with the use of in vitro models to detect human DILI: integrated risk assessment and mitigation plans. *BioMed Research International*, 2016, 9737920. <https://doi.org/10.1155/2016/9737920>.
- Carletti, E., Colletier, J. P., Dupeux, F., Trovaslet, M., Masson, P., & Nachon, F. (2010). Structural evidence that human acetylcholinesterase inhibited by tabun ages through O-dealkylation. *Journal of Medicinal Chemistry*, 53(10), 4002-4008. <https://doi.org/10.1021/jm901853b>.
- Cheung, J., Rudolph, M., Burshteyn, F., Cassidy, M., Gary, E., Love, J., Franklin, M., & Height, J. (2012). Structures of human acetylcholinesterase in complex with pharmacologically important ligands. *Journal of Medicinal Chemistry*, 55(22), 10282–10286.

<https://doi.org/10.1021/jm300871x>.

- de Almeida, J. S. F. D., Cavalcante, S. F. A., Dolezal, R., Kuca, K., Musilek, K., Jun, D., & França, T. C. C. (2019). Molecular modeling studies on the interactions of aflatoxin B1 and its metabolites with the peripheral anionic site of human acetylcholinesterase. *Journal of Biomolecular Structure and Dynamics*, 37(8), 2041-2048. <https://doi.org/10.1080/07391102.2018.1475259>.
- Dvir, H., Silman, I., Harel, M., Rosenberry, T., & Sussman, J. (2010). Acetylcholinesterase: From 3D structure to function. *Chemico-Biological Interactions*, 187(1-3), 10-22. <https://doi.org/10.1016/j.cbi.2010.01.042>.
- Ece, A. (2020). Towards more effective acetylcholinesterase inhibitors: a comprehensive modelling study based on human acetylcholinesterase protein-drug complex. *Journal of Biomolecular Structure and Dynamics*, 38(2), 565-572. <https://doi.org/10.1080/07391102.2019.1583606>.
- Ece, A., & Sevin, F. (2010). Exploring QSAR on 4-cyclohexylmethoxypyrimidines as antitumor agents for their inhibitory activity of CDK2. *Letters in Drug Design & Discovery*, 7(9), 625-631. <https://doi.org/10.2174/157018010792929612>.
- Eckert, A., Keil, U., Marques, C., Bonert, A., Frey, C., Schüssel, K., & Müller, W. (2003). Mitochondrial dysfunction, apoptotic cell death, and Alzheimer's disease. *Biochemical Pharmacology*, 66(8), 1627-1634. [https://doi.org/10.1016/S0006-2952\(03\)00534-3](https://doi.org/10.1016/S0006-2952(03)00534-3).
- Ellman, G., Courtney, K., Andres, V., & Featherstone, R. (1961). A new and rapid colorimetric determination of acetylcholinesterase activity. *Biochemical Pharmacology*, 7(2), 88-95. [https://doi.org/10.1016/0006-2952\(61\)90145-9](https://doi.org/10.1016/0006-2952(61)90145-9).
- Eslami, M., Nezafat, N., Negahdaripour, M., & Ghasemi, Y. (2019). Computational approach to suggest a new multi-target-directed ligand as a potential medication for Alzheimer's disease. *Journal of Biomolecular Structure and Dynamics*, 37(18), 4825-4839. <https://doi.org/10.1080/07391102.2018.1564701>.
- Han, L., Lai, P., & Du, J.-R. (2014). Deciphering molecular mechanism underlying hypolipidemic activity of echinocystic acid. *Evidence-Based Complementary and Alternative Medicine*, 2014, 1-7. <https://doi.org/10.1155/2014/823154>.
- Harel, M., Kleywegt, G. J., Ravelli, R. B., Silman, I., & Sussman, J.L. (1995). Crystal structure of an acetylcholinesterase-fasciculin complex: interaction of a three-fingered toxin from snake venom with its target. *Structure*, 3(12), 1355-1366. [https://doi.org/10.1016/s0969-2126\(01\)00273-8](https://doi.org/10.1016/s0969-2126(01)00273-8).

- Harel, M., Quinn, D., Nair, H., Silman, I., & Sussman, J. (1996). The X-ray structure of a transition state analog complex reveals the molecular origins of the catalytic power and substrate specificity of acetylcholinesterase. *Journal of the American Chemical Society*, 118(10), 2340-2346. <https://doi.org/10.1021/ja952232h>.
- Itteboina, R., Ballu, S., Sivan, S. & Manga, V. (2017). Molecular modeling-driven approach for identification of Janus kinase 1 inhibitors through 3D-QSAR, docking and molecular dynamics simulations. *Journal of Receptors and Signal Transduction*, 37(5), 453-469. <https://doi.org/10.1080/10799893.2017.1328442>.
- Jin, Z., Yang, L., Liu, S.-J., Wang, J., Li, S., Lin, H.-Q., Wan, D., & Hu, C. (2010a). Synthesis and biological evaluation of 3,6-diaryl-7H-thiazolo[3,2-b][1,2,4]triazin-7-one derivatives as acetylcholinesterase inhibitors. *Archives of Pharmacal Research*, 33(10), 1641–1649. <https://doi.org/10.1007/s12272-010-1013-8>.
- Jin, Z., Yang, L., Xu, X. N., Huang, E. R., Wan, D. C. Li, S., Huang, H. Q., & Hu, C. (2010b). Synthesis and biological activity of 3,6-diaryl-7H-thiazolo[3,2-b][1,2,4]triazin-7-one derivatives as novel acetylcholinesterase inhibitors. *Science China Chemistry*, 53(11), 2297-2303. <https://doi.org/10.1007/s11426-010-4094-9>.
- Kangueane, P., & Nilofer, C. (2018). *Patented Protein Structural Complexes in Discovery Platform*. In: *Protein-Protein and Domain-Domain Interactions*. Springer, Singapore. https://doi.org/10.1007/978-981-10-7347-2_17.
- Khalid, A., Zaheer-ul-Haq, Anjum, S., Khan, M., Atta-ur-Rahman, & Choudhary, M. (2004). Kinetics and structure–activity relationship studies on pregnane-type steroidal alkaloids that inhibit cholinesterases. *Bioorganic & Medicinal Chemistry*, 12(9), 1995-2003. <https://doi.org/10.1016/j.bmc.2004.03.002>.
- Khan, M., Fuskevåg, O.-M., & Sylte, I. (2009). Discovery of potent thermolysin inhibitors using structure based virtual screening and binding assays. *Journal of Medicinal Chemistry*, 52(1), 48-61. <https://doi.org/10.1021/jm8008019>.
- Kryger, G., Silman, I., & Sussman, J. (1999). Structure of acetylcholinesterase complexed with E2020 (Aricept): implications for the design of new anti-Alzheimer drugs. *Structure*, 7(3), 297-307. [https://doi.org/10.1016/S0969-2126\(99\)80040-9](https://doi.org/10.1016/S0969-2126(99)80040-9).
- Liu, S., Shang, R., Shi, L., Wan, D., & Lin, H. (2014). Synthesis and biological evaluation of

7*H*-thiazolo[3,2-*b*]-1,2,4-triazin-7-one derivatives as dual binding site acetylcholinesterase inhibitors. *European Journal of Medicinal Chemistry*, 81, 237-244. <https://doi.org/10.1016/j.ejmech.2014.05.020>.

Liu, S.-J., Cui, L.-B., Xu, H.-L., Wang, T.-Y., Hu, C., Li, S., Lin, H.-Q., & Wan, D. (2013). Design, synthesis, and biological evaluation of 7*H*-thiazolo[3,2-*b*]-1,2,4-triazin-7-one derivatives as dual binding site acetylcholinesterase inhibitors. *Heterocycles*, 87(12), 2607-2614. <https://doi.org/10.3987/COM-13-12820>.

Liu, S.-J., Yang, L., Jin, Z., Huang, E.-F., Wan, D., Lin, H.-Q., & Chun H. (2009). Design, synthesis, and biological evaluation of 7*H*-thiazolo[3,2-*b*]-1,2,4-triazin-7-one derivatives as novel acetylcholinesterase inhibitors. *ARKIVOC*, (x), 333-348. <https://doi.org/10.3998/ark.5550190.0010.a30>.

Liu, S.-J., Yang, L., Liu, X.-G., Luo, Y., Cao, Z.-J., Wan, D., Lin, H.-Q., & Hu, C. (2010). Design, synthesis, and biological evaluation of 7*H*-thiazolo[3,2-*b*]-1,2,4-triazin-7-one derivatives as acetylcholinesterase inhibitors. *Letters in Drug Design & Discovery*, 7(1), 5-8. <https://doi.org/10.2174/157018010789869343>.

Malinak, D., Dolezal, R., Hepnarova, V., Hozova, M., Andrys, R., Bzonek, P., Racakova, V., Korabecny, J., Gorecki, L., Mezeiova, E., Psocka, M., Jun, D., Kuca, K., & Musilek, K. (2020). Synthesis, in vitro screening and molecular docking of isoquinolinium-5-carbaldoximes as acetylcholinesterase and butyrylcholinesterase reactivators. *Journal of Enzyme Inhibition and Medicinal Chemistry*, 35(1), 478-488. <https://doi.org/10.1080/14756366.2019.1710501>.

Marvel, C., & Schertz, G. (1943). Copolymers of *p*-chlorostyrene and methyl methacrylate. *Journal of the American Chemical Society*, 65(11), 2054-2058. <https://doi.org/10.1021/ja01251a006>.

Mosmann, T. (1983). Rapid colorimetric assay for cellular growth and survival: Application to proliferation and cytotoxicity assays. *Journal of Immunological Methods*, 65(1-2), 55-63. [https://doi.org/10.1016/0022-1759\(83\)90303-4](https://doi.org/10.1016/0022-1759(83)90303-4).

Muñoz-Ruiz, P., Rubio, L., García-Palomero, E., Dorronsoro, I., del Monte-Millán, M., Valenzuela, R., Usán, P., de Austria, C., Bartolini, M., Andrisano, V., Bidon-Chanal, A., Orozco, M., Luque, F., Medina, M., & Martínez, A. (2005). Design, synthesis, and biological evaluation of dual binding site acetylcholinesterase inhibitors: new disease-modifying agents for Alzheimer's disease. *Journal of Medicinal Chemistry*, 48(23), 7223-7233.

<https://doi.org/10.1021/jm0503289>.

National Medical Products Administration. The National Medical Products Administration conditional approved GV-971 as the mild to moderate Alzheimer's disease drug. [2019-11-09].

<http://www.nmpa.gov.cn/WS04/CL2056/359779.html>.

Neto, D., Lima, J., de Almeida, J., França, T., Nascimento, C., & Villar, J. (2017). New semicarbazones as gorge-spanning ligands of acetylcholinesterase and potential new drugs against Alzheimer's disease: Synthesis, molecular modeling, NMR, and biological evaluation. *Journal of Biomolecular Structure and Dynamics*, 1-15. <https://doi.org/10.1080/07391102.2017.1407676>.

Pascoini, A. L., Federico, L. B., Arêas, A. L. F., Verde, B. A., Freitas P. G., & Camps, I. (2019). In silico development of new acetylcholinesterase inhibitors. *Journal of Biomolecular Structure and Dynamics*, 37(4), 1007-1021. <https://doi.org/10.1080/07391102.2018.1447513>.

Polinsky, R. (1998). Clinical pharmacology of rivastigmine: a new-generation acetylcholinesterase inhibitor for the treatment of alzheimer's disease. *Clinical Therapeutics*, 20(4), 634-647. [https://doi.org/10.1016/S0149-2918\(98\)80127-6](https://doi.org/10.1016/S0149-2918(98)80127-6).

Raves, M., Harel, M., Pang, Y.-P., Silman, I., Kozikowski, A., & Sussman, J. (1997). Structure of acetylcholinesterase complexed with the nootropic alkaloid, (-)-huperzine A. *Nature Structural & Molecular Biology*, 4(1), 57-63. <https://doi.org/10.1038/nsb0197-57>.

Rego, A., & Oliveira, C. (2003). Mitochondrial dysfunction and reactive oxygen species in excitotoxicity and apoptosis: implications for the pathogenesis of neurodegenerative diseases. *Neurochemical Research*, 28(10), 1563-1574. <https://doi.org/10.1023/A:1025682611389>.

Shamsi, A., Al Shahwan, M., Ahamad, S., Hassan, M. I., Ahmad, F., & Islam, A. (2020). Spectroscopic, calorimetric and molecular docking insight into the interaction of Alzheimer's drug donepezil with human transferrin: implications of Alzheimer's drug. *Journal of Biomolecular Structure and Dynamics*, 38(4), 1094-1102. <https://doi.org/10.1080/07391102.2019.1595728>.

Shiri, F., Pirhadi, S., & Ghasemi, J. B. (2019). Dynamic structure based pharmacophore modeling of the Acetylcholinesterase reveals several potential inhibitors. *Journal of Biomolecular Structure and Dynamics*, 37(7), 1800-1812. <https://doi.org/10.1080/07391102.2018.1468281>.

Shivakumar, D., Williams, J., Wu, Y., Damm, W., Shelley, J. & Sherman, W. (2010). Prediction of

absolute solvation free energies using molecular dynamics free energy perturbation and the OPLS force field. *Journal of Chemical Theory and Computation*, 6(5), 1509-1519. <https://doi.org/10.1021/ct900587b>.

Śledź, P., & Caflisch, A. (2018). Protein structure-based drug design: from docking to molecular dynamics. *Current Opinion in Structural Biology*, 48, 93-102. <https://doi.org/10.1016/j.sbi.2017.10.010>.

Sussman, J., Harel, M., Frolow, F., Oefner, C., Goldman, A., Toker, L., & Silman, I. (1991). Atomic structure of acetyl-cholinesterase from *Torpedo californica*: a prototypic acetylcholine-binding protein. *Science*, 253(5022), 872-879. <https://doi.org/10.1126/science.1678899>.

Taft, C., da Silva, V., & da Silva, C. (2008). Current topics in computer-aided drug design. *Journal of Pharmaceutical Sciences*, 97(3), 1089-1098. <https://doi.org/10.1002/jps.21293>.

Tahtaci, H., Karacık, H., Ece, A., Er, M., & Şeker, M. (2017). Design, synthesis, SAR and molecular modeling studies of novel imidazo[2,1-b][1,3,4]thiadiazole derivatives as highly potent antimicrobial agents. *Molecular Informatics*, 37(3), 1700083. <https://doi.org/10.1002/minf.201700083>.

Vaqué, M., Ardévol, A., Bladé, C., Salvadó, M., Blay, M., Fernández-Larrea J., Arola, L., & Pujadas, G. (2008). Protein-ligand docking: a review of recent advances and future perspectives. *Current Pharmaceutical Analysis*, 4(1), 1-19. <https://doi.org/10.2174/157341208783497597>.

Wan, Y.-F., Guan, S.-S., Qian, M.-D., Huang, H.-H., Han, F., Wang, S., & Zhang, H. (2020). Structural basis of fullerene derivatives as novel potent inhibitors of protein acetylcholinesterase without catalytic active site interaction: insight into the inhibitory mechanism through molecular modeling studies. *Journal of Biomolecular Structure and Dynamics*, 38(2), 410-425. <https://doi.org/10.1080/07391102.2019.1576543>.

Wang, M., Li, W., Wang, Y., Song, Y., Wang, J., & Cheng, M. (2018). In silico insight into voltage-gated sodium channel 1.7 inhibition for anti-pain drug discovery. *Journal of Molecular Graphics and Modelling*, 84, 18-28. <https://doi.org/10.1016/j.jm gm.2018.05.006>.

Xu, H., Jin, Z., Liu, S., Liu, H., Li, S., Lin, H., Wan, D., & Hu, C. (2012). Design, synthesis characterization and in vitro biological activity of a series of 3-aryl-6-(bromoarylmethyl)-7H-thiazolo[3,2-b]-1, 2, 4-triazin-7-one derivatives as the novel acetylcholinesterase inhibitors. *Chinese Chemical Letters*, 23(7), 765-768.

<https://doi.org/10.1016/j.ccllet.2012.04.022>.

Yang, S. Y. (2010). Pharmacophore modeling and applications in drug discovery: challenges and recent advances. *Drug Discovery Today*, 2010, 15(11-12):444-450.

<https://doi.org/10.1016/j.drudis.2010.03.013>.

Zheng, H., Fridkin, M., & Youdim, M. B. (2010). Site-activated chelators derived from anti-Parkinson drug rasagiline as a potential safer and more effective approach to the treatment of Alzheimer's disease. *Neurochemical Research*, 35(12), 2117-23.

<https://doi.org/10.1007/s11064-010-0293-1>.

Zhu, J., Wang, Y., Li, X., Han, W., & Zhao, L. (2017). Understanding the interactions of different substrates with wild-type and mutant acylaminoacyl peptidase using molecular dynamics simulations. *Journal of biomolecular Structure & Dynamics*, 36(16), 1-43.

<https://doi.org/10.1080/07391102.2017.1414634>.

Accepted Manuscript

Figure 1. The amino acid residues of *Tc*AChE active site (a. left, 1FSS), *hA*ChE active site (b. right, 2X8B). CAS for green, PAS for blue violet, and QABS for deep pink.

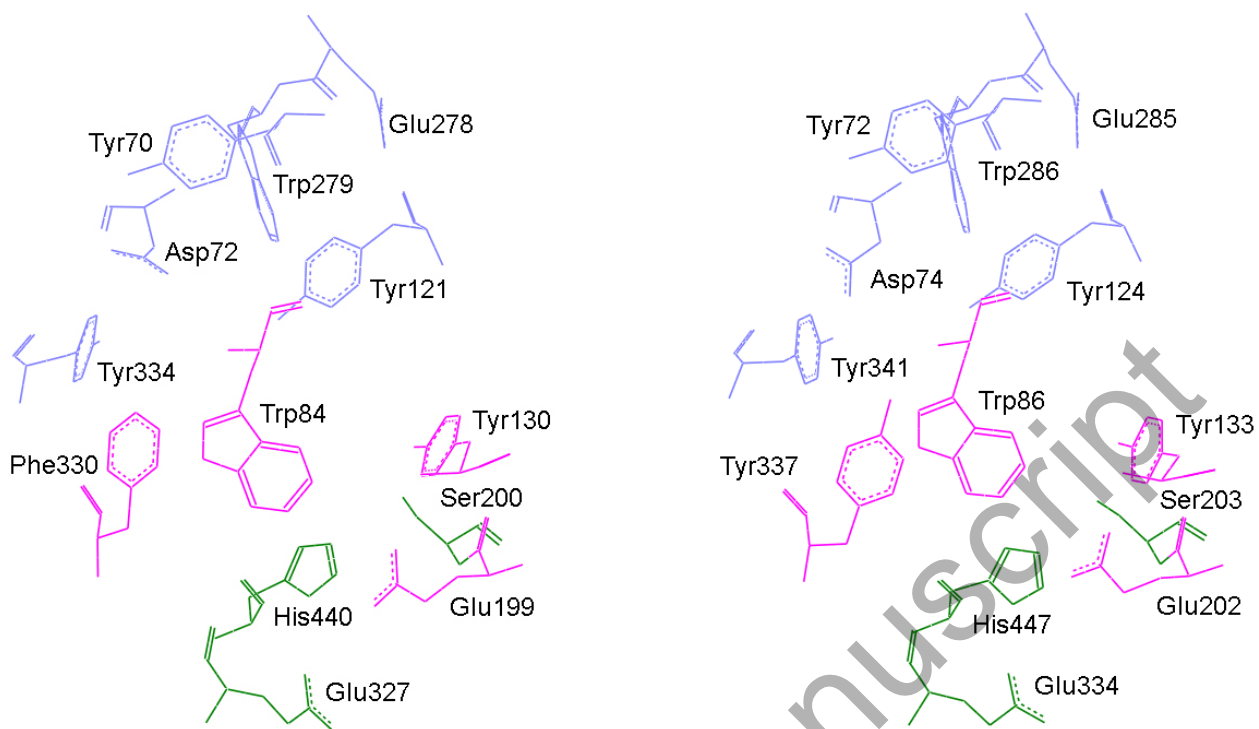


Figure 2. The overlapping conformations of the native ligand and the docking ligand of 4EY7.

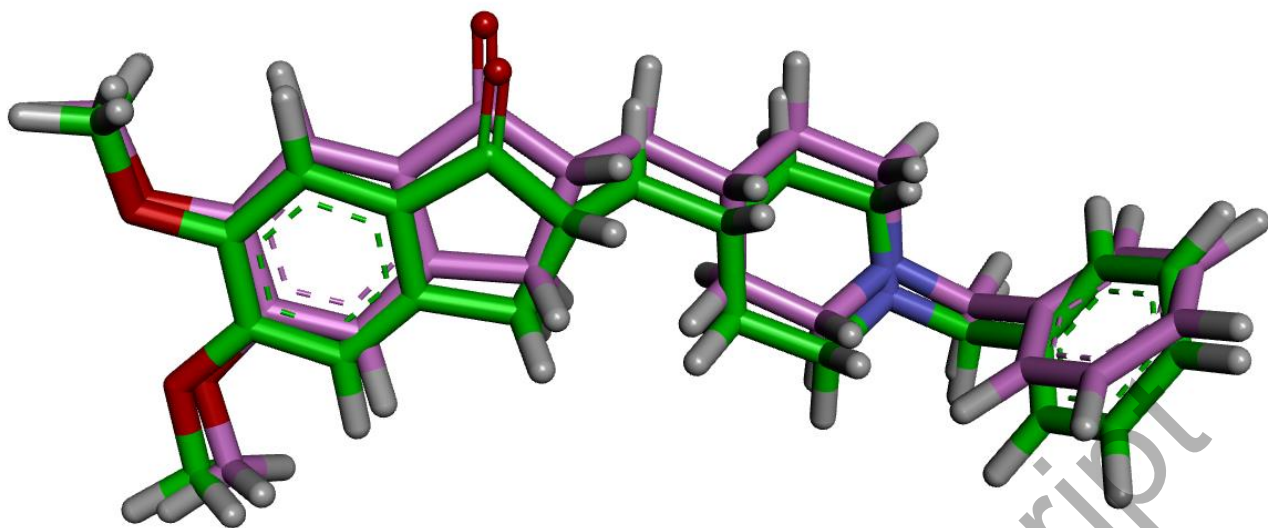
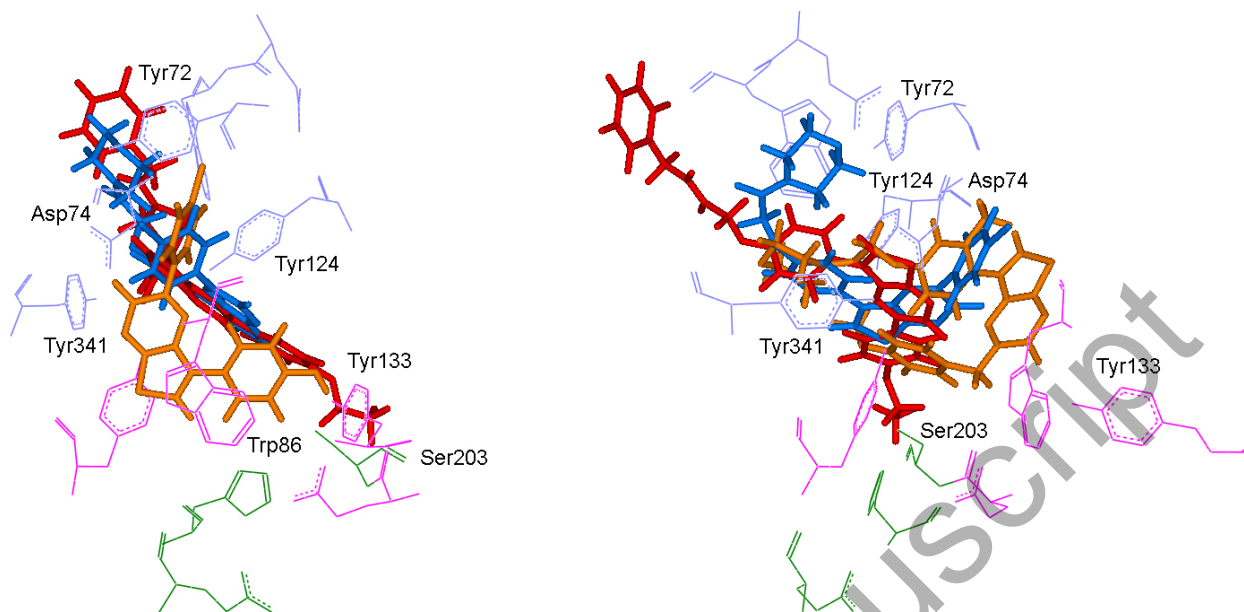


Figure 3. Compounds **4a**, **10g**, **4d** in the *hAChE* active sites (PDB code: 2X8B) (a. left, viewed along the “gorge”; b. right, viewed clearly different active sites). CAS for green, PAS for blue violet, QABS for deep pink. Compound **4a** for red, **4d** for blue, **10g** for dark orange.



Accepted Manuscript

Figure 4. The highly active compounds in the *hAChE* active sites (PDB code: 2X8B)

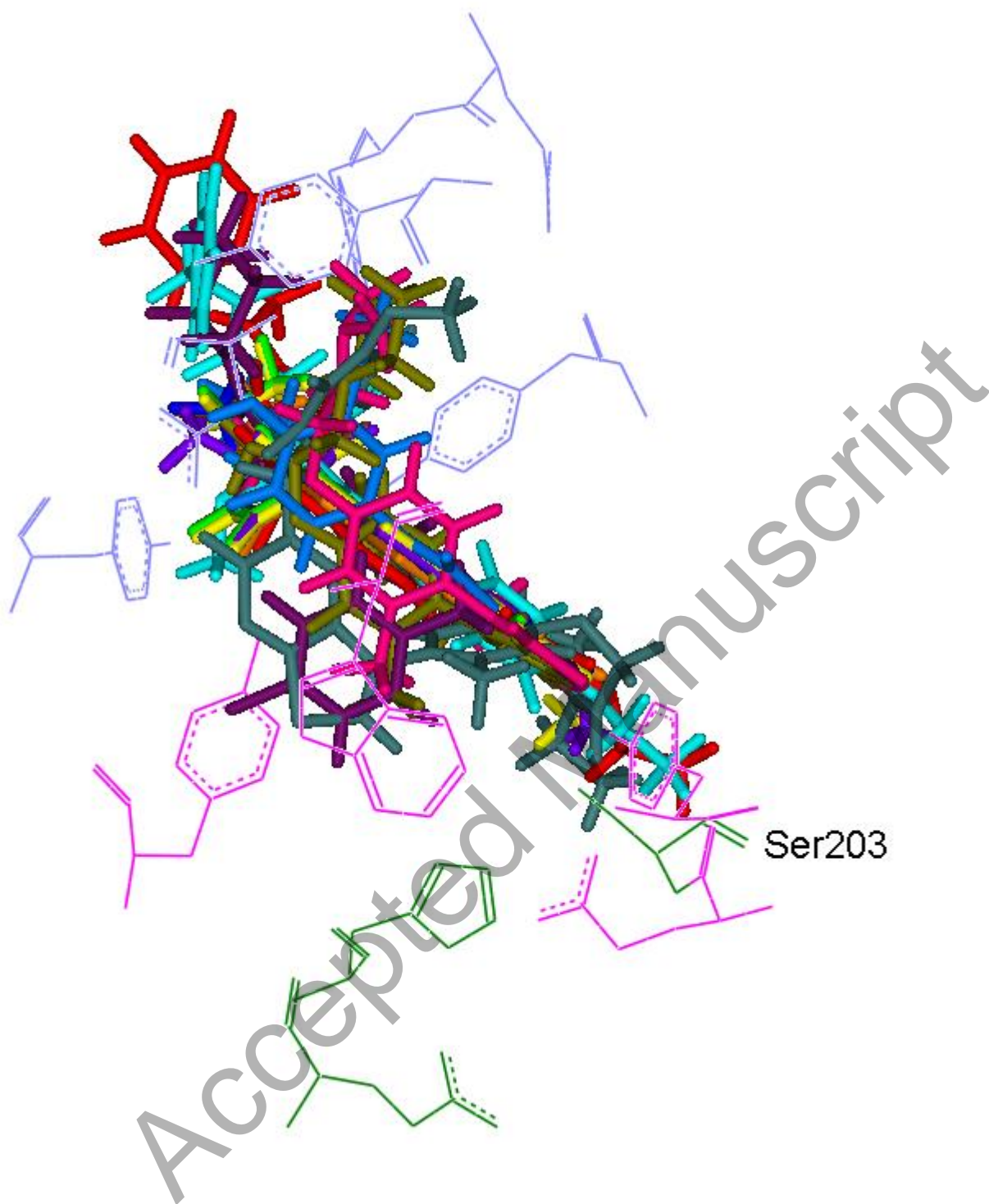


Figure 5. The moderately active compounds in the *hAChE* active sites (PDB code: 2X8B)

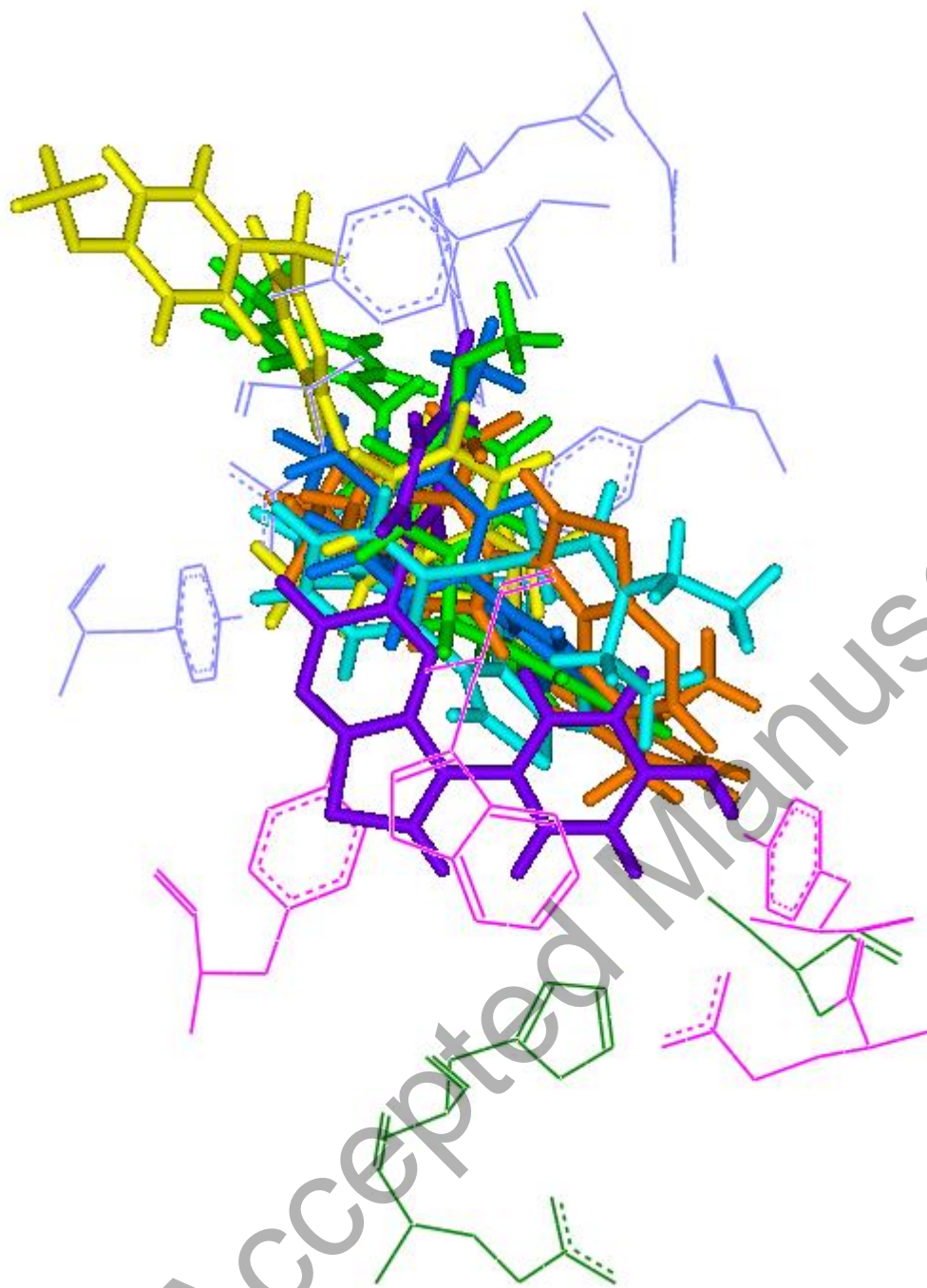
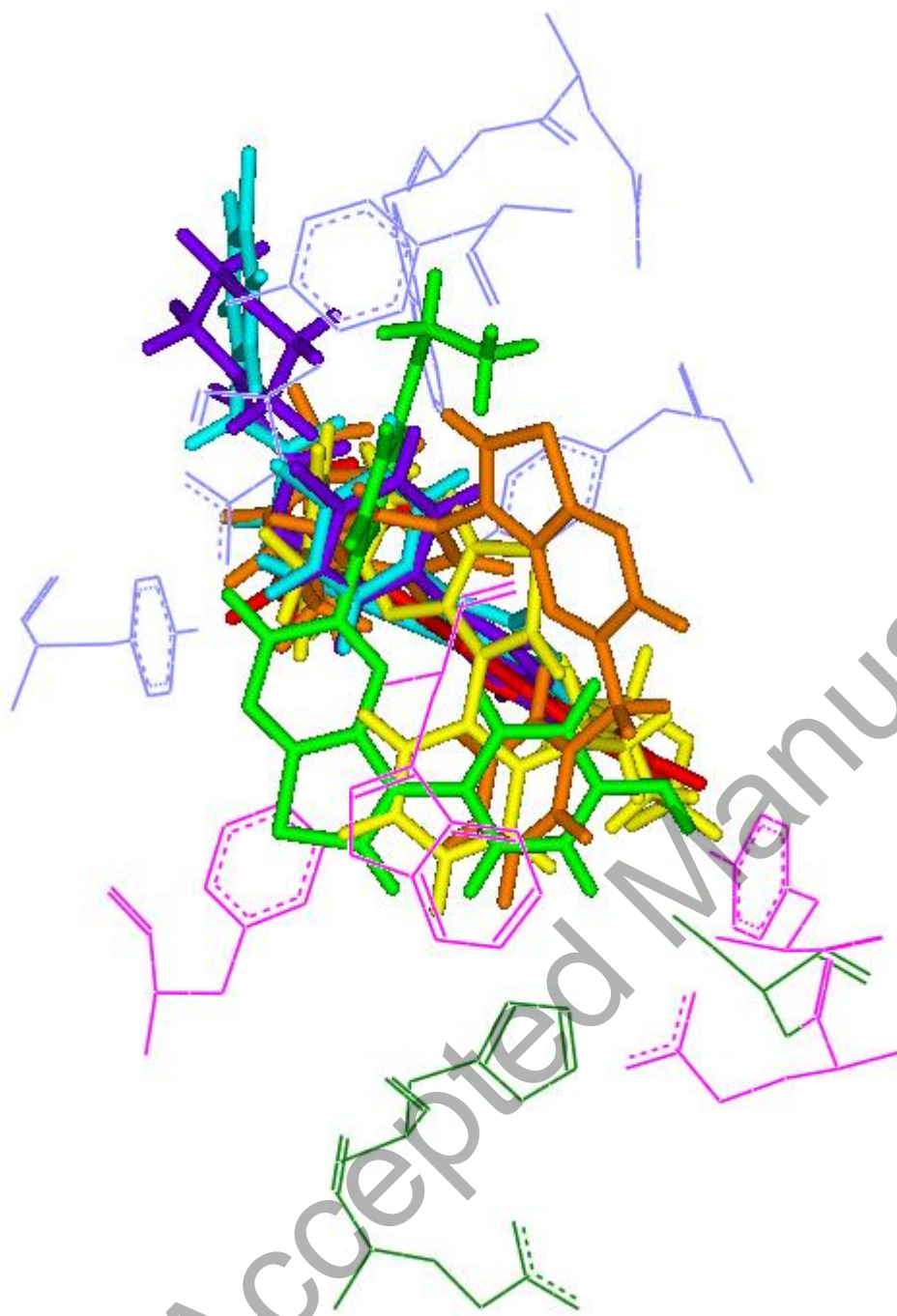
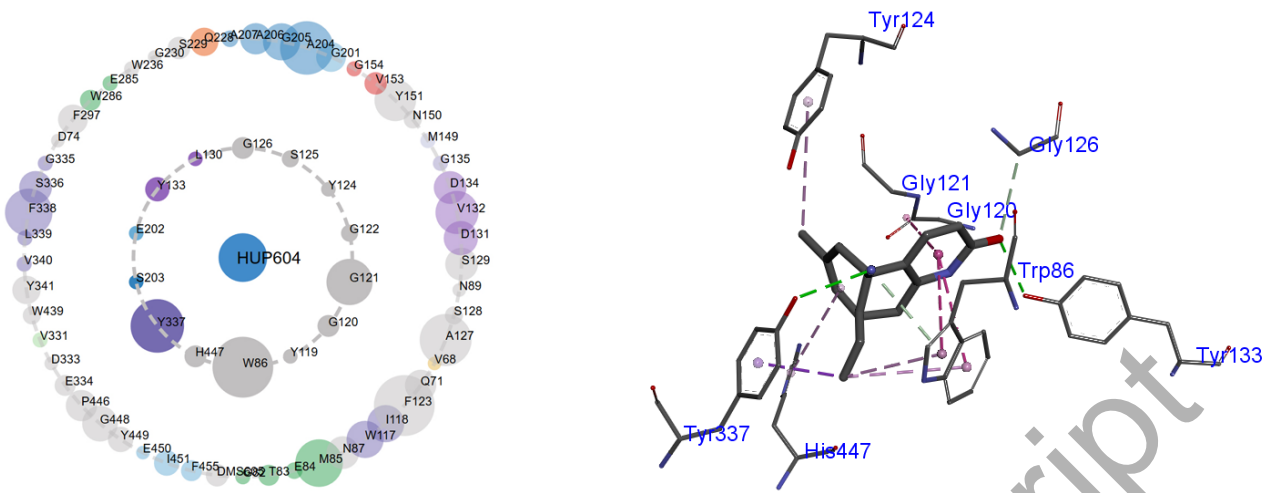


Figure 6. The inactive compounds in the *h*AChE active sites (PDB code: 2X8B)



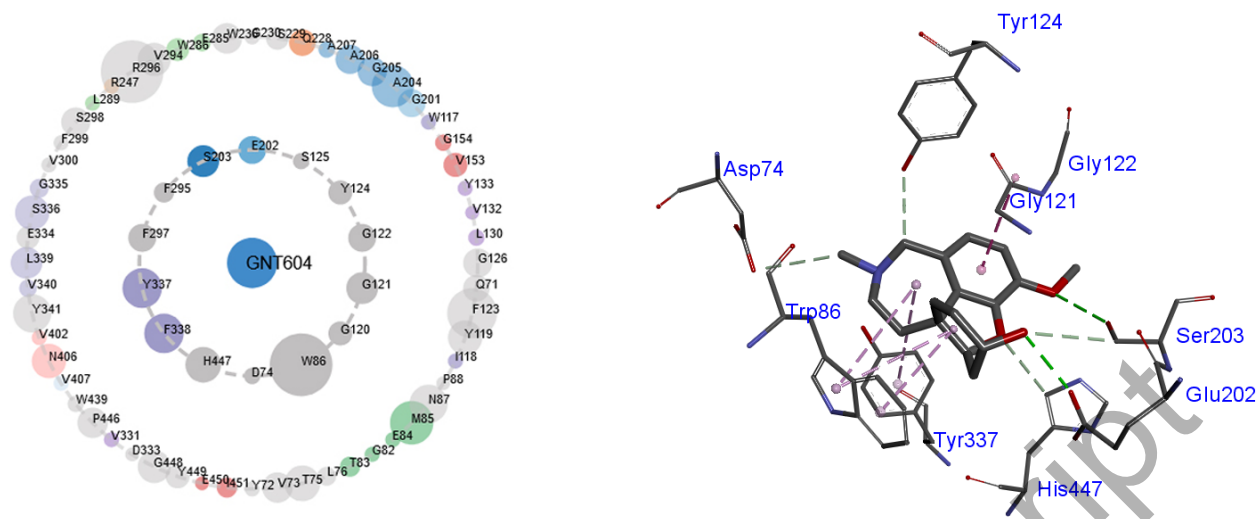
Accepted Manuscript

Figure 7. The asteroid plot (left) and binding interaction (right) of (-)-huperzine A at the active sites of *hAChE* (PDB code: 4EY5).



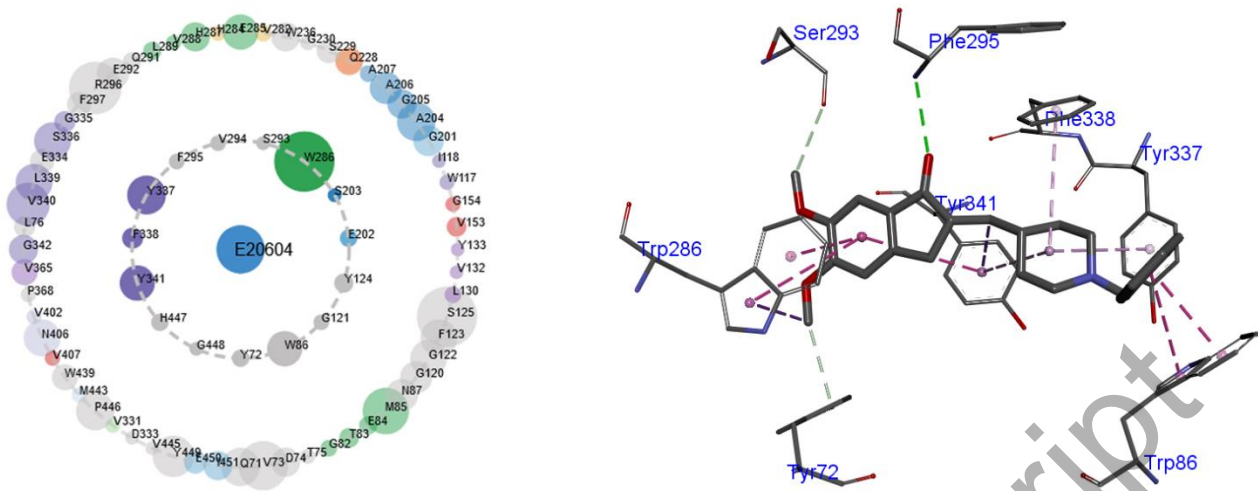
Accepted Manuscript

Figure 8. The asteroid plot (left) and binding interaction (right) of (-)-galantamine at the active sites of *hAChE* (PDB code: 4EY6).



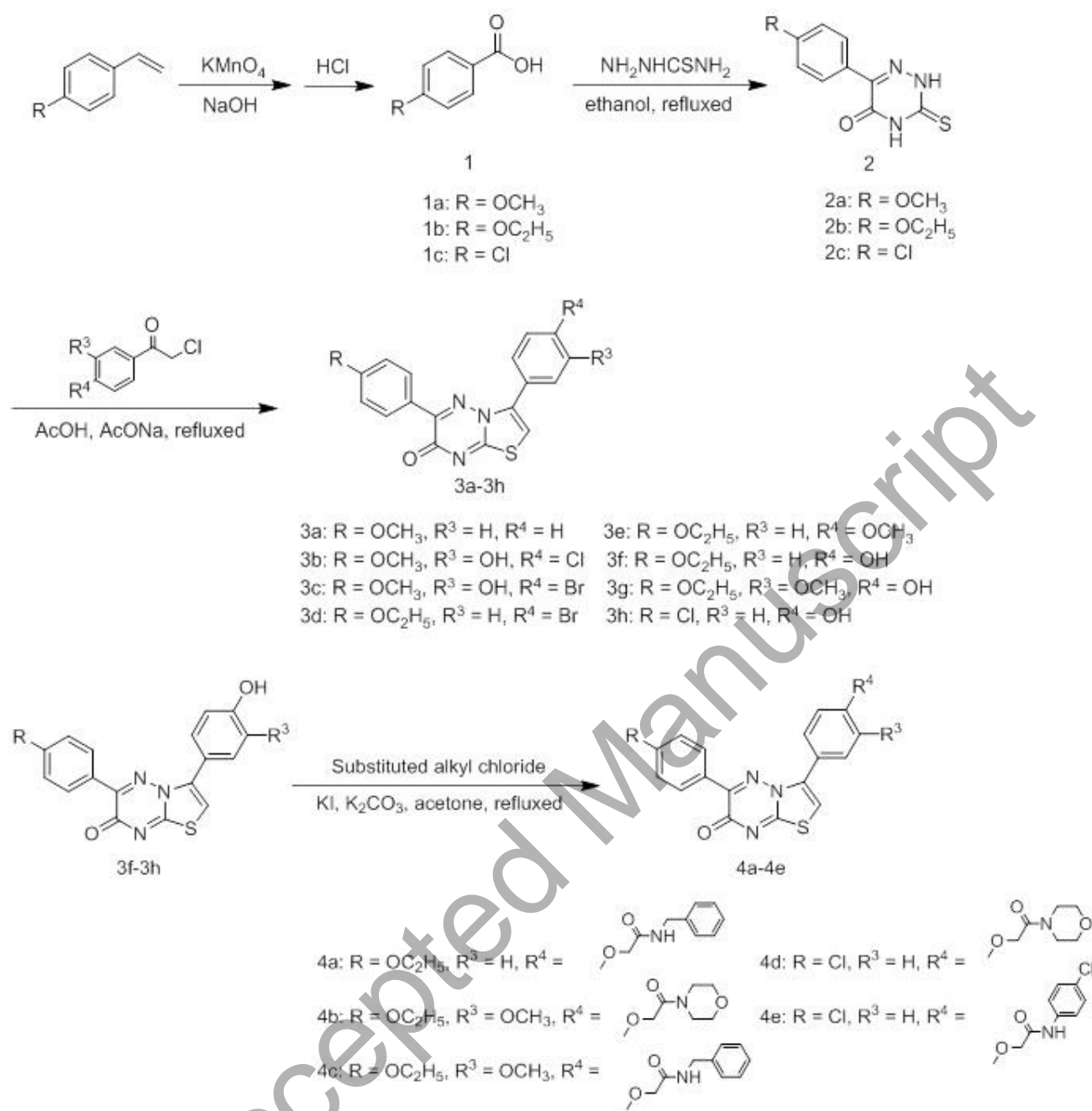
Accepted Manuscript

Figure 9. The asteroid plot (left) and binding interaction (right) of donepezil at the active sites of *hAChE* (PDB code: 4EY7).

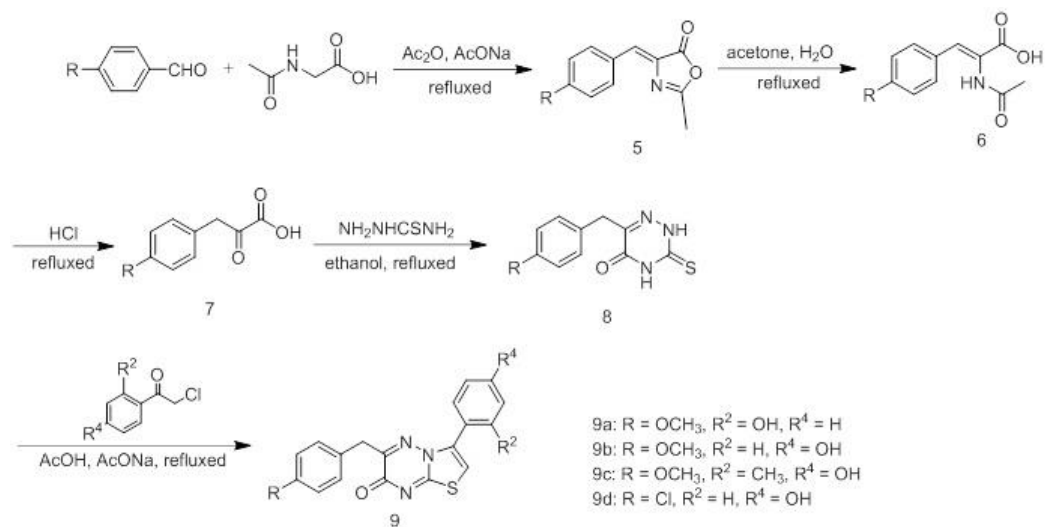


Accepted Manuscript

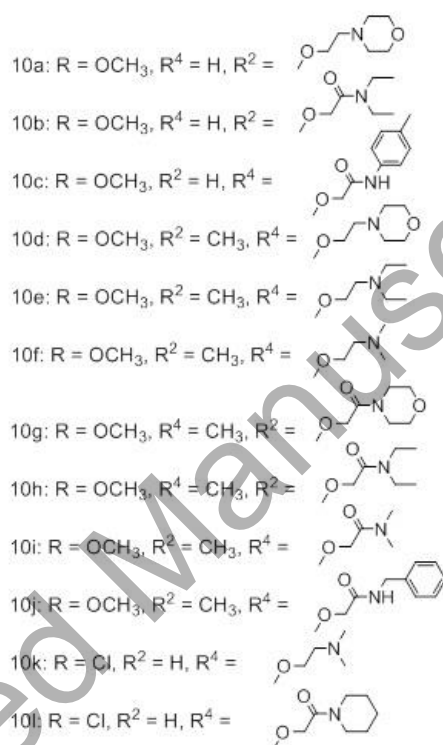
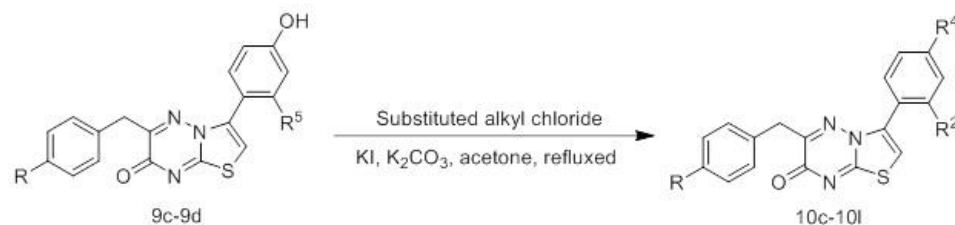
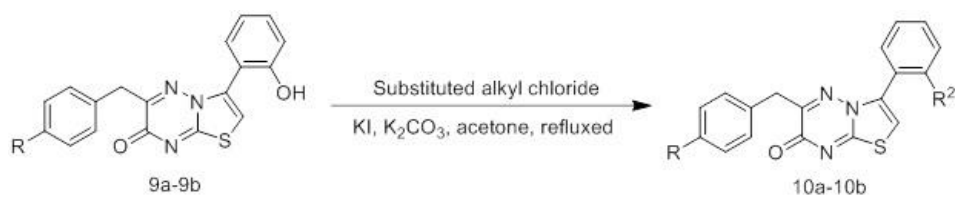
Scheme 1. The synthetic route of **3a-3h** and **4a-4e**



Scheme 2. The synthetic route of **9a-9d** and **10a-10l**



Accepted Manuscript



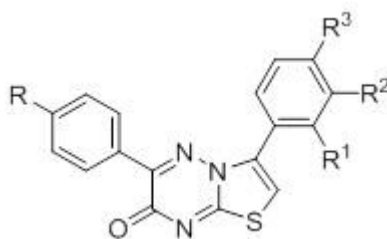
Accepted Manuscript

Table 1. Different inhibitors interacted with different active sides of the AChE

AChE Inhibitor	Amino acid Residues	Active Sites
tacrine (Raves, et al., 1997)	His440	CAS
	Asp72	PAS
donepezil (Cheung, et al., 2012)	Trp279	PAS
	Trp84, Phe330	QABS
rivastigmine (Polinsky, 1998)	Ser200	CAS
huperzine A (Raves, et al., 1997)	His440	CAS
	Trp84, Tyr130	QABS
	Glu199, Phe330	QABS

Accepted Manuscript

Table 2. The substituent groups list of the target compounds



No.	R	R ¹	R ²	R ³	Yield, %	mp, °C
3a	methoxy	hydrogen	hydrogen	hydrogen	56.7	216-218
3b	methoxy	hydrogen	hydroxy	chloro	38.7	279-281
3c	methoxy	hydrogen	hydroxy	bromo	37.8	268-270
3d	ethoxy	hydrogen	hydrogen	bromo	48.1	265-267
3e	ethoxy	hydrogen	hydrogen	methoxy	18.3	230-232
3f	ethoxy	hydrogen	hydrogen	hydroxy	42.8	202-205
3g	ethoxy	hydrogen	methoxy	hydroxy	60.5	239-241
3h	chloro	hydrogen	hydrogen	hydroxy	12.9	237-238
4a	ethoxy	hydrogen	hydrogen	(2-benzylamino)-2-oxoethoxy	44.1	146-148
4b	ethoxy	hydrogen	methoxy	2-morpholinyl-2-oxoethoxy	49.9	258-260
4c	ethoxy	hydrogen	methoxy	(2-benzylamino)-2-oxoethoxy	67.1	216-218
4d	chloro	hydrogen	hydrogen	2-morpholinyl-2-oxoethoxy	56.3	158-160
4e	chloro	hydrogen	hydrogen	2-(4-chlorobenzylamino)-2-oxoethoxy	31.3	138-141
9a	methoxy	hydroxy	hydrogen	hydrogen	72.8	218-219
9b	methoxy	hydrogen	hydrogen	hydroxy	62.7	188-189
9c	methoxy	methyl	hydrogen	hydroxy	61.4	192-194
9d	chloro	hydrogen	hydrogen	hydroxy	65.4	219-221
10a	methoxy	2-(4-morpholinyl)ethoxy	hydrogen	hydrogen	52.2	160-162
10b	methoxy	(2-diethylamino)-2-oxoethoxy	hydrogen	hydrogen	45.9	165-166

10c	methoxy	hydrogen	hydrogen	2-(4-methylphenylamino)-2-oxoethoxy	38.0	213-215
10d	methoxy	methyl	hydrogen	2-(4-morpholinyl)ethoxy	33.5	180-182
10e	methoxy	methyl	hydrogen	(2-diethylamino)ethoxy	37.6	134-136
10f	methoxy	methyl	hydrogen	(2-dimethylamino)ethoxy	36.6	143-144
10g	methoxy	2-(4-morpholinyl)-2-oxoethoxy	hydrogen	methyl	40.4	119-120
10h	methoxy	(2-diethylamino)-2-oxoethoxy	hydrogen	methyl	38.6	149-151
10i	methoxy	methyl	hydrogen	(2-dimethylamino)-2-oxoethoxy	32.3	117-119
10j	methoxy	methyl	hydrogen	(2-benzylamino)-2-oxoethoxy	35.1	214-215
10k	chloro	hydrogen	hydrogen	(2-dimethylamino)ethoxy	40.8	189-190
10l	chloro	hydrogen	hydrogen	2-(1-piperidinyl)-2-oxoethoxy	41.4	203-205

Accepted Manuscript

Table 3. The *hAChE* inhibitory activity values of the target compounds

No.	Inhibition,%	No.	Inhibition,%
3a	3.70	3b	73.97
3c	75.41	3d	58.63
3e	65.73	3f	3.29
3g	46.04	3h	54.85
4a	58.12	4b	27.34
4c	77.19	4d	10.65
4e	25.00	9a	64.36
9b	62.43	9c	73.97
9d	56.29	10a	29.48
10b	41.21	10c	40.02
10d	66.37	10e	71.72
10f	64.25	10g	43.20
10h	64.57	10i	61.22
10j	43.68	10k	70.73
10l	75.69		

note: Inhibitory ratio of huperzine-A at 10 μ M ($n = 3$) was 100%.

Table 4. The hydrogen bond interaction sites of the highly active compounds (PDB code: 2X8B)

No.	Inhibition,%	Interaction Sites	Active Sites
3b	73.97	Ser203, Tyr124	CAS, PAS
3c	75.41	Ser203, Tyr124	CAS, PAS
3d	58.63	Ser203, Tyr124	CAS, PAS
3e	65.73	Ser203, Tyr124	CAS, PAS
4a	58.12	Ser203, Tyr124, Tyr341	CAS, PAS
4c	77.19	Ser203, Tyr124	CAS, PAS
9a	64.36	Ser203, Tyr124	CAS, PAS
9b	62.43	Ser203, Trp86, Tyr72, Asp74	CAS, QABS, PAS
9c	73.97	Ser203, Trp86, Tyr72, Asp74	CAS, QABS, PAS
9d	56.29	Ser203, Tyr72, Asp74	CAS, PAS
10d	66.37	Ser203, Tyr72, Tyr124	CAS, PAS
10e	71.72	Ser203, Trp86	CAS, QABS
10f	64.25	Ser203, Tyr124, Tyr341	CAS, PAS
10h	64.57	Ser203, Trp86	CAS, QABS
10i	61.22	Ser203, Trp86	CAS, QABS
10k	70.73	Ser203, Trp86	CAS, QABS
10l	75.69	Ser203, Trp86	CAS, QABS

Table 5. The hydrogen bond interaction sites of the moderately active compounds (PDB code: 2X8B)

No.	Inhibition (%)	Interaction Sites	Active Sites
3g	46.04	Asp74, Tyr124	PAS
3h	54.85	Trp86, Tyr133, Asp74	QABS, PAS
10b	41.21	Trp86, Tyr124	QABS, PAS
10c	40.02	Asp74, Tyr124	PAS
10g	43.20	Tyr133, Tyr124, Tyr341	QABS, PAS
10j	43.68	Tyr124	PAS

Accepted Manuscript

Table 6. The hydrogen bond interaction sites of the inactive compounds (PDB code: 2X8B)

No.	Inhibition, %	Interaction Sites	Active Sites
3a	3.70	Tyr124, Tyr341	PAS
3f	3.29	Trp86, Asp74, Tyr124	QABS, PAS
4b	27.34	Tyr124, Tyr341	PAS
4d	10.65	Tyr72, Asp74, Tyr124	PAS
4e	25.00	Asp74, Tyr124	PAS
10a	29.48	Asp74	PAS

Accepted Manuscript

Table 7. The hydrogen bonds interaction sites of the highly active compounds (PDB code: 4EY7)

No.	Inhibition, %	Hydrogen Bond Interaction at Site	Active Site	Other Interactions Site
3b	73.97	Ser203	CAS	Tyr341
3c	75.41	Ser203	CAS	Tyr341
3d	58.63	Ser203	CAS	Trp286, Tyr341
3e	65.73	—	—	Ser203; Trp286, Tyr341
4a	58.12	Ser203; Asp74	CAS, PAS	Trp86, Tyr337; Asp74, Tyr124
4c	77.19	Ser203; Glu202; Asp74	CAS, QABS, PAS	Trp86, Tyr133, Glu202, Tyr337; Asp74
9a	64.36	Ser203	CAS	Trp86, Glu202, Tyr337; Tyr124
9b	62.43	Tyr133, Tyr337; Tyr124	QABS, PAS	Trp86; Asp74
9c	73.97	Ser203	CAS	Trp86, Tyr337; Tyr124
9d	56.29	Ser203; Tyr337; Tyr341	CAS, QABS, PAS	Trp86, Tyr337
10d	66.37	Ser203; Tyr133	CAS, QABS	Asp74, Trp286
10e	71.72	Ser203; Tyr337	CAS, QABS	Trp86, Tyr133, Tyr337; Tyr124
10f	64.25	Ser203; Tyr133	CAS, QABS	Trp86
10h	64.57	Ser203	CAS	Tyr337; Trp286, Tyr341
10i	61.22	Ser203	CAS	Trp286
10k	70.73	Trp86	QABS	Trp86, Tyr337; Asp74, Tyr124, Tyr341
10l	75.69	—	—	His447; Trp86, Tyr337; Tyr124, Tyr341

note: the amino acid residues located in different active sites were separated by the semicolons

Table 8. The hydrogen bond interaction sites of the moderately active compounds (PDB code: 4EY7)

No.	Inhibition, %	Hydrogen Bond Interaction Site	Active Site	Other Interactions Site
3g	46.04	Asp74	PAS	Trp86, Tyr337; Asp74, Tyr124
3h	54.85	Glu202; Asp74	QABS, PAS	Trp86, Tyr337; Asp74, Tyr124
10b	41.21	Tyr337; Tyr124	QABS, PAS	Trp86, Glu202, Tyr337; Tyr124
10c	40.02	Tyr337; Tyr124	QABS, PAS	Trp86, Tyr337; Asp74
10g	43.20	Tyr133; Tyr341	QABS, PAS	Trp286, Tyr341
10j	43.68	Tyr124	PAS	Trp86, Tyr337; Asp74

notes: the amino acid residues located in different active sites were separated by the semicolons

Table 9. The hydrogen bonds interaction sites of the target compounds (PDB code: 4EY7)

No.	Inhibition, %	Hydrogen Bond Interaction Sites	Active Site	Other Interaction Site
3a	3.70	Tyr341	PAS	Tyr337; Asp74, Tyr124
3f	3.29	Glu202; Asp74	QABS, PAS	Trp86, Glu202, Tyr337; Asp74
4b	27.34	Tyr124	PAS	Tyr337; Asp74, Tyr124, Tyr341
4d	10.65	Asp74	PAS	Trp86, Tyr337; Tyr72, Asp74, Tyr124
4e	25.00	Trp86; Asp74	QABS, PAS	Trp86, Tyr337; Asp74, Tyr124
10a	29.48	Tyr124	PAS	Trp86, Glu202, Tyr337; Asp74, Tyr124, Tyr341

notes: the amino acid residues located in different active sites were separated by semicolons